JOURNAL OF CATALYSIS **178,** 598–603 (1998)
ARTICLE NO. CA982206

Evidence for Enhanced Dissociation of CO on Rh/Ceria

E. S. Putna,* R. J. Gorte,* J. M. Vohs,*,[1] and G. W. Graham†

*Department of Chemical Engineering, University of Pennsylvania, Philadelphia, Pennsylvania 19104; and †Chemical and Physical Sciences Laboratory, Ford Motor Company, Mail Drop 3179, Building SRL, P.O. Box 2053, Dearborn, Michigan 48121-2053

Received June 2, 1998; revised June 4, 1998; accepted June 4, 1998

The adsorption and reaction of CO on Rh particles supported on oxidized and partially reduced epitaxial ceria films on yttria-stabilized cubic zirconia (YSZ) (100), (110), and (111) single crystals was studied using temperature-programmed desorption (TPD) and X-ray photoelectron spectroscopy (XPS). The ceria films on YSZ were highly reducible, reacting with CO adsorbed on Rh particles to produce CO_2 during TPD. After reduction of the ceria, however, the CO TPD results contained two features: a low-temperature state resulting from desorption of molecular CO and a high-temperature state resulting from the recombination of C and O atoms produced by CO dissociation at lower temperature. The fraction of CO which dissociated on YSZ-supported Rh/ceria increased with the extent of reduction of the ceria surface. TPD studies with isotopically labeled CO demonstrated that the O atoms produced by CO dissociation undergo exchange with oxygen from the ceria lattice. The CO dissociation reaction was found to be metal specific and was not observed for either Pd or Pt supported on reduced ceria/YSZ.

INTRODUCTION

It is well known that ceria provides oxygen storage capacity (OSC) in three-way automotive catalysts and is important in maintaining oxidation activity during fuel-rich operating conditions (1–4). In a series of investigations, we have examined the mechanism by which ceria provides oxygen for reaction with CO adsorbed on supported Rh and the interactions between ceria and zirconia which enhance this process (5,16). We have previously demonstrated that this process is highly structure sensitive. For example, during TPD of CO-dosed Rh supported on CeO_2(111) and CeO_2(100) single crystal surfaces, less than 2% of the adsorbed CO is oxidized to CO_2 (7). In contrast, in similar experiments using ceria thin films supported on α-Al_2O_3(0001) and polycrystalline zirconia, as much as 20% of the adsorbed CO is oxidized to CO_2 (16). We have also recently observed an unusually high activity for CO dissociation on Rh supported on partially reduced CeO_2(111) and CeO_2(100) single-crystal surfaces (8).

In the work reported here we have extended our previous studies to include model catalysts composed of Pt, Pd, and Rh supported on epitaxial films of CeO_2 grown on single crystal surfaces of yttria-stabilized zirconia (YSZ). The goals of this study were to further elucidate the effect of zirconia–ceria interactions on oxidation activity, to determine the nature of the Rh-ceria interactions that result in enhanced activity for CO dissociation, and to determine if the dissociation pathway is specific to Rh.

EXPERIMENTAL TECHNIQUES

The experimental setup used for the TPD measurements in this study was identical to that described previously (10) and consisted of an ion-pumped vacuum chamber with a cylindrical-mirror analyzer for Auger electron spectroscopy and a quadrupole mass spectrometer. Samples were exposed to $^{16}O_2$, $^{12}C^{16}O$, or $^{13}C^{18}O$ (Isotec Inc., 99.03 at% ^{13}C, 97.3 at% ^{18}O), using directed beam dosers in order to maintain a low base pressure. The pressure in front of the dosers has been estimated to be approximately 20 times higher than the background chamber pressure during dosing, and quoted exposures were calculated using this factor. TPD measurements were carried out with a linear heating rate of 10 K/s. XPS measurements were performed in a separate UHV chamber at Ford Research Laboratory using a Physical Electronics double-pass CMA and Mg(Kα) X-ray source which has been described previously (11).

The oxide substrates consisted of $10 \times 10 \times 0.5$-mm YSZ crystals (9.5 mol% Y) oriented to expose the (100), (111), or (110) surface. The crystals were obtained from Aithaca Chemical Corp. and their surface orientation was confirmed using Laue X-ray diffraction. For all orientations, the alignment was within 1° of the desired crystal plane. The crystals were mounted in Ta foil holders that enabled them to be resistively heated to 900 K. The temperature was monitored using a chromel–alumel thermocouple attached to the back surface using ceramic adhesive (Aremco 516).

The YSZ substrates were cleaned by Ar^+ ion bombardment (1.5 kV, 5 μA sample current) at 300 K. They were then annealed in 10^{-7} torr of O_2 at 800 K for 10 min, followed by oxidation in 10^{-7} torr O_2 at 450 K for 30 min.

[1] Corresponding author.

0021-9517/98 $25.00

Following this cleaning procedure, a CeO_2 film was deposited by evaporating Ce metal (Johnson Matthey, 99.9%) onto the substrate held at 450 K in the presence of 10^{-7} Torr of O_2. Following ceria deposition, the samples were oxidized in 10^{-7} Torr of O_2 for 15 min at 450 K to ensure complete oxidation of the Ce metal. Rh, Pt, or Pd was subsequently vapor deposited onto the substrate at 300 K. The coverage of the precious metal and CeO_2 films was determined using a quartz crystal, film-thickness monitor.

RESULTS

As described in previous studies of ceria films on zirconia (12), the ceria films on the YSZ single crystals were reducible. This is demonstrated in the TPD results for CO on $Rh/CeO_2/YSZ(100)$ displayed in Fig. 1a. This data was obtained using a saturation exposure of CO on $2 \times 10^{15} Rh/cm^2$ supported on a ceria film, approximately 4 nm in thickness. In this experiment, the sample was heated to 600 K following deposition of the Rh, prior to exposing it to CO, in order to ensure Rh particle formation. Based on dispersion measurements using CO (13), the average Rh particle size for this sample was ~3.5 nm.

As shown in Fig. 1a, a significant fraction of the adsorbed CO desorbs as CO_2. Based on the peak area for CO (m/e = 28) and CO_2 (m/e = 44), approximately 70% of the adsorbed CO reacts between 300 and 500 K to form CO_2 in this initial TPD experiment. Note that CO does not adsorb on ceria/YSZ(100) in the absence of a precious metal (7) and CO_2 was not formed in TPD studies of CO from Rh/YSZ(100) in the absence of ceria (14). Therefore, the results in Fig. 1a demonstrate that, on these model catalysts, CO adsorbed on the Rh can react with lattice oxygen from the ceria. Note also that the fraction of adsorbed CO oxidized to CO_2 is significantly higher than that observed for Rh on ceria films supported on polycrystalline zirconia.

In subsequent CO TPD measurements, the total amount of CO that adsorbed, as measured by the combined areas of the CO and CO_2 features, remained approximately constant, and the ratio of CO to CO_2 increased until practically no CO_2 was observed for a completely reduced ceria film as shown in Fig. 1b. Similar CO TPD experiments were also carried out using a sample for which the ceria film was reduced by heating to 900 K prior to deposition of the Rh. The results of these experiments were identical to those displayed in Fig. 1b.

The data in Fig. 1b also show that, in addition to a decrease in the amount of CO_2 produced, as the ceria film became increasingly reduced, a new, high-temperature CO desorption feature appears at 625 K. The intensity of this peak increased with the degree of reduction of the ceria support. This result is similar to that observed in CO TPD studies for Rh supported on reduced $CeO_2(111)$ and $CeO_2(100)$, where CO dissociation has been shown to occur (7,8). Note, however, that ion sputtering and/or high temperature annealing was required to reduce the single crystal surfaces, while, for the CeO_2/YSZ system studied here, reduction could be accomplished by reaction with CO.

Displayed in Fig. 1c is the TPD result for a saturation exposure of $^{13}C^{18}O$ on the Rh/ceria/YSZ(100) sample following 10 adsorption–desorption cycles, with heating to 800 K. The TPD data show two CO features at 500 and 625 K, with the low-temperature feature being primarily $^{13}C^{18}O$ and the high-temperature feature primarily $^{13}C^{16}O$. Other possible products such as CO_2, $^{12}C^{16}O$, or $^{12}C^{18}O$ were not observed from this reduced sample. Subsequent TPD curves were identical to the ones shown here. The appearance of the high-temperature CO desorption feature was found to be reversible, and it disappeared after the sample was reoxidized in 10^{-7} torr of O_2 at 600 K. The isotopic composition of the high-temperature CO peak demonstrates that a portion of the adsorbed CO dissociates on the reduced

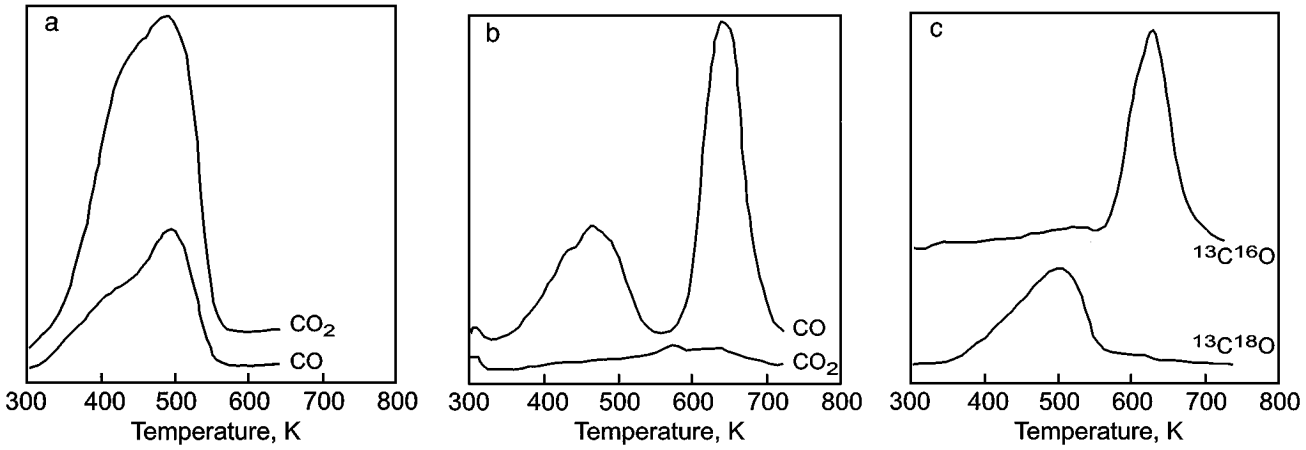

FIG. 1. TPD data obtained following $^{12}C^{16}O$ adsorption at 300 K on Rh supported on (a) a fully oxidized ceria film on YSZ(100), (b) a partially reduced ceria film on YSZ(100), and (c) following $^{13}C^{18}O$ adsorption at 300 K on Rh supported on a partially reduced ceria film on YSZ(100).

Rh/ceria/YSZ(100) sample and that oxygen from the dissociated CO exchanges with lattice oxygen from the reduced ceria film, similar to what was reported for Rh on reduced CeO_2(111) and CeO_2(100) single crystals (7,8).

The surface carbon species corresponding to the high-temperature feature is relatively unreactive, as demonstrated by the following experiment. After reduction of Rh/ceria/YSZ(100), the sample was exposed to CO at 300 K and heated to 550 K, a temperature sufficient to desorb the molecular CO but low enough to maintain the high-temperature state. Upon cooling to 300 K, the sample was exposed to a saturation dose of O_2, followed by a saturation dose of CO. Subsequent TPD data contained a high-temperature CO desorption feature, equal in intensity to that observed in previous CO desorption measurements on reduced Rh/ceria/YSZ(100). CO and CO_2 peaks were observed below 500 K as well; however, the total amount of CO and CO_2 desorbing at the lower temperatures was essentially the same as the amount of CO which desorbed below 500 K in Fig. 1b. These observations are consistent with the surface of Rh being covered with carbon atoms which prevent adsorption of oxygen.

It is important to note that the high-temperature state for CO desorption was not observed in earlier studies of the reaction of CO on Rh supported on polycrystalline ceria films, regardless of the extent of the ceria reduction (6, 15, 16). Furthermore, since the ceria films in the present study were relatively thick, ~4 nm, it seems unlikely that any electronic interactions at the CeO_2-YSZ substrate would affect reactivity. Since the CeO_2 films grow epitaxially on the YSZ(100) surface (9), the YSZ does, however, significantly influence the structure of the CeO_2 layer. Therefore, these possible structural effects were further investigated using YSZ(111) and YSZ(110) substrates. As noted above, previous work by Dmowski *et al.* has shown that ceria films grow epitaxially on all three YSZ surfaces used in this study (9). Thus, changing the crystallographic orientation of the YSZ support allowed the crystallographic orientation of the ceria surface to be systematically varied. The TPD results obtained using the YSZ(111) and YSZ(110) supports were indistinguishable from those using YSZ(100). Even though the activity for CO dissociation is strongly dependent on the ceria structure, the surface crystallographic orientation does not appear to be important, at least for low-index planes.

The influence of both Rh and ceria thickness was also examined. TPD experiments were performed for Rh supported on ceria films with average thicknesses of 0.4, 4, and 20 nm. For the 0.4 and 4 nm ceria films, Rh coverages of 0.25×10^{15} and 3.0×10^{16} Rh/cm^2, corresponding to average Rh particle sizes of 1.6 and 10.0 nm, were examined. The samples were reduced by heating in 10^{-7} torr of CO at 800 K for 10 min. In all cases, CO TPD data obtained after this treatment were similar to those shown in Fig. 1b.

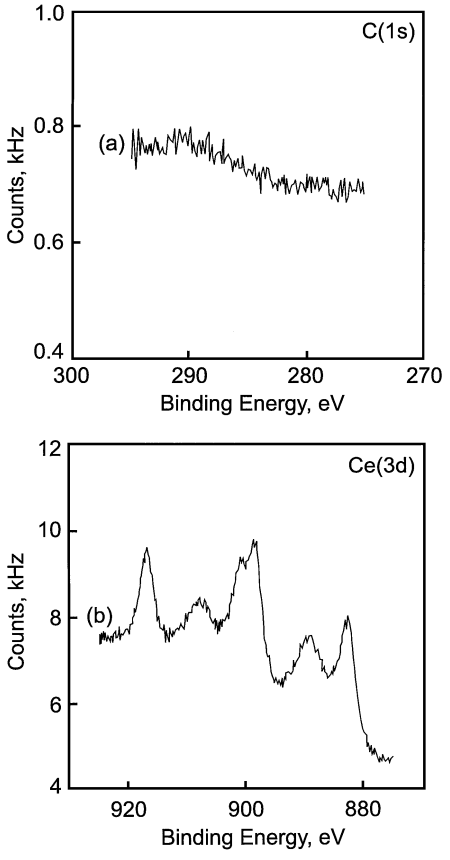

FIG. 2. XPS spectra for Rh supported on fully oxidized ceria on YSZ(111). Spectrum (a) corresponds to the C(1s) region, while spectrum (b) corresponds to the Ce(3d) region.

Typically, between 60 and 80% of the adsorbed CO dissociated on the reduced Rh/ceria/YSZ(100) samples and no CO_2 was observed on any of the reduced samples.

In order to provide additional insight into the nature of both the Rh and the adsorbed CO, a Rh/ceria/YSZ(111) sample was characterized using XPS. Samples for the XPS experiments were prepared following the same basic procedure as those used for the TPD measurements, except that film thicknesses were estimated from the attenuation of the substrate photoemission signal. Figure 2 shows the C(1s) and Ce(3d) spectra obtained from a 3.5-nm ceria film upon which approximately 0.5×10^{15} Rh/cm^2 had been deposited, prior to adsorption of CO. The broad feature in the spectrum of the C(1s) region is not due to C(1s) electrons but rather results mostly from photoemission from the Ce(4s) state, together with weak structure from the Rh($3d_{5/2}$) state induced by Mg($K\alpha_{5,6}$) X-rays (note that the primary Rh($3d_{5/2}$) peak induced by Mg($K\alpha_{1,2}$) X-rays appears at 307 eV). The Ce(3d) spectrum contains a two spin-orbit split, partially overlapping broad regions of three peaks located between 882 and 916 eV. This spectrum is similar to that reported previously for both polycrystalline and single crystalline CeO_2 and is characteristic of Ce^{+4} (7,17).

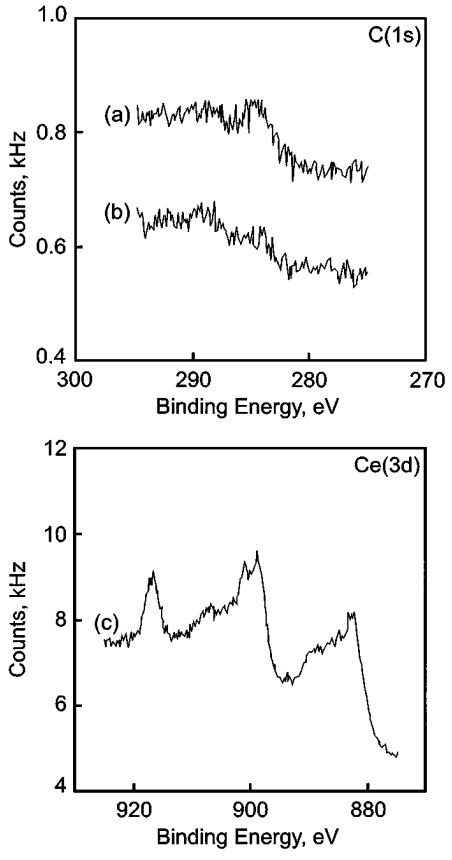

FIG. 3. XPS spectra obtained following exposure of Rh supported on partially reduced ceria on YSZ(111) to a saturation dose of CO. The upper panel corresponds to the C(1s) region (a) after dosing CO and (b) after heating the sample in (a) to 573 K. The lower panel corresponds to the Ce(3d) of the reduced sample.

The complexity of the spectrum results from final state effects. A complete assignment of the various peaks can be found in papers by Creaser *et al.* (17).

After annealing the sample at 573 K in 1×10^{-8} torr of CO for 600 s, it was dosed with 1×10^{-8} torr of CO for 600 s at 300 K. Spectrum a in Fig. 3 corresponds to the C(1s) spectrum obtained after this treatment, while spectrum b was obtained after heating the CO-dosed sample to 573 K. The spectrum obtained after dosing at 300 K contains a broad peak centered at 285 eV, a part of which can be assigned to molecularly adsorbed CO. Heating the CO-dosed sample to 573 K resulted in attenuation of the peak due to molecularly adsorbed CO at 285 eV (curve b, in Fig. 3a), but left a peak at 284 eV. This peak can be assigned to carbon atoms formed via the dissociation of adsorbed CO.

The Ce(3d) spectrum of the reduced sample is shown in Fig. 3c. The intensity of the primary photoemission peaks associated with Ce^{+4} cations, i.e. 898 eV and 916 eV, is significantly attenuated and the spectrum is characteristic of a mixture of Ce^{+4} and Ce^{+3} in partially reduced ceria (17). Based on the peak shapes and comparison to the work of Creaser *et al.* (17), the data indicate that approximately 25% of the Ce cations are in the +3 oxidation state. Reduction did not produce any changes in the Rh(3d) spectrum, however. The Rh($3d_{5/2}$) peak appeared at 307 eV for both the oxidized and reduced samples and is consistent with zero-valent Rh.

The effect of changing the precious metal from Rh to Pt or Pd on the ceria/YSZ(100) support was also investigated. In previous work on CeO_2(111) and CeO_2(100) single crystals, it was found that, unlike the case with Rh, CO dissociation does not occur on supported Pt and Pd particles following reduction (18). The same result was observed in the present study of YSZ-supported ceria. Only the results for Pd will be shown here, but the results for Pt were essentially identical.

Figure 4a displays TPD data for CO desorption from a Pd/ceria/YSZ(100) sample prepared in a manner identical to that for which results are shown in Fig. 1, except that 2×10^{15} Pd/cm^2 was deposited instead of Rh. Following

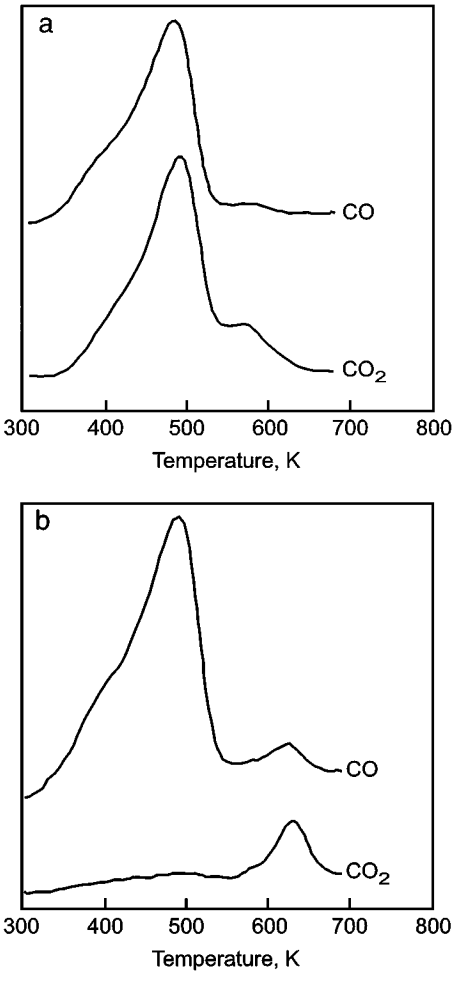

FIG. 4. TPD data obtained following CO adsorption at 300 K on Pd supported on (a) fully oxidized ceria on YSZ(100) and (b) on partially reduced ceria on YSZ(100).

sample preparation, CO was adsorbed to saturation at 300 K. During TPD, CO desorbed in a peak centered at 500 K with a shoulder to lower temperatures, while CO_2 desorbed between 350 K and 600 K. With the exception that slightly less CO was converted to CO_2 in the first TPD experiment using Pd, the CO TPD results for the supported Pd and Rh on the oxidized films were similar. Figure 4b shows the CO TPD data after reduction of the Pd/ceria/YSZ(100) sample at 573 K in 1×10^{-8} torr CO for 600 s. Both CO (m/e 28) and CO_2 (m/e 44) desorbed in peaks centered at 500 K, with shoulders to lower temperatures. Note that small CO and CO_2 peaks are evident at 625 K. The size of the high-temperature CO peak, however, was significantly smaller for reduced Pd/ceria/YSZ(100) relative to that for reduced Rh/ceria/YSZ(100). Furthermore, similar, high-temperature features for CO and CO_2 are present in the TPD curves for the oxidized Pd/ceria/YSZ(100) sample, although at a slightly lower temperature. Therefore, it is likely that the high-temperature features for Pd/ceria/YSZ(100) are experimental artifacts, possibly due to reaction of adventitious carbon or carbonate impurities. XPS results support this conclusion, since C(1s) spectra from reduced Pd/ceria/YSZ(111) did not provide evidence for surface carbon after heating to 573 K.

In summary, CO dissociation occurs readily on highly reduced Rh catalysts supported on model ceria/YSZ supports. Among the precious metals typically used in automotive catalysis, this reactivity is unique to Rh and does not occur on supported Pt or Pd.

DISCUSSION

The results of this study demonstrate that Rh supported on partially reduced, epitaxial films of ceria on YSZ(100), YSZ(111), and YSZ(110) exhibits unusually high activity for CO dissociation. This result is consistent with that reported for Rh supported on reduced CeO_2(111) and CeO_2(100) surfaces (7,8). The enhanced reactivity for CO dissociation appears to be specific to Rh. Appreciable amounts of CO dissociation were not observed for either Pd or Pt on similar supports. Since CO does not interact strongly with the ceria under the conditions of our experiments, it is clear that the dissociation reaction takes place on the Rh or at the Rh-ceria interface. Surprisingly, the fraction of CO which dissociates does not depend on Rh particle size for particles up to 10 nm in diameter. Although the thickness of the ceria films on the YSZ crystals did not influence the results, the structure of these films was important, since dissociation was not enhanced for Rh on polycrystalline ceria films grown in a manner similar to those examined here, but supported on alumina (16). While there are similarities in our findings with Rh to reports for CO dissociation on small Pd particles (<5 nm) (19–21), the effect in our study is clearly caused by a different mechanism.

Several possibilities can be proposed to account for the dramatic increase in the CO dissociation activity of Rh upon partial reduction of the ceria support, although none are entirely satisfactory. First, it is possible that reduction of the ceria produces a change in the morphology of the supported Rh particles and thereby exposes Rh sites that are active for CO dissociation. Several reports in the literature indicate that highly stepped Rh surfaces exhibit activity for CO dissociation, so that morphological changes in the Rh could explain enhanced dissociation (22,23). On the other hand, in studies of Rh single crystals, less than 10% of the adsorbed CO typically dissociates, in marked contrast to our observation of as much as 80% dissociation. Furthermore, the TPD experiments in this study do not provide evidence for a change in the Rh particle size or morphology upon reduction of the support. Accounting for the fact that some of the CO desorbed as CO_2 on the oxidized sample, the total area of the CO TPD peaks were nearly the same for Rh supported on both oxidized and reduced ceria/YSZ films. Taking these factors into account, an explanation based entirely on a change in the morphology of the Rh particles upon reduction of the ceria does not appear to account for the large increase in CO dissociation activity.

A second possibility to account for enhanced CO dissociation on the reduced Rh/ceria/YSZ samples is that reaction occurs at the Rh-ceria interface, with sites from both phases participating. In this case, migration of the adsorbed oxygen atoms formed during CO dissociation from the Rh to the reduced ceria could provide a driving force for the dissociation reaction. Support for this mechanism comes from FTIR studies, which have identified CO species that bond with the carbon end of the molecule attached to Rh while the oxygen interacts with a Ce^{+3} cation (24). Species of this type have an unusually low ν(CO) stretching frequency, $\sim$1695 cm^{-1}, due to transfer of electron density into CO antibonding orbitals. This frequency is at the low end of the range characteristic of a C-O double bond. A reduction in the C-O bond order for these species would imply that they are prime candidates for dissociation. A mechanism of this type might also explain why CO_2 is not produced during CO desorption measurements. Ordinarily, one would expect a Rh surface with substantial coverages of both CO and oxygen (formed by CO dissociation) to form CO_2 very rapidly, leaving some carbon on the surface. However, we did not observe either CO_2 or carbon deposits in multiple TPD experiments, suggesting that oxygen atoms must have a very short residence time on the Rh.

The chief difficulty with this picture is that it cannot easily account for the invariance in the percentage of CO which undergoes dissociation with Rh particle size. If dissociation occurs at interfacial sites, one would expect this percentage to decrease with increasing Rh particle size, even if carbon resulting from dissociation were able to rapidly diffuse to the rest of the surface. This mechanism also provides

no explanation for why Pt and Pd are different from Rh, nor does it explain why the structure of ceria should be important.

A variation on the Rh–ceria interface mechanism involves formation of a partially oxidized Rh species in contact with ceria. It can be argued that the adsorptive properties of CO will be influenced by electronic interactions between Rh and ceria in this case and that the properties for supported Rh could be very different from those of Pt or Pd. The idea that a reaction could occur between Rh and ceria seems quite likely, given that Rh reacts with lanthanide oxides to produce stable perovskites (25). Although the present XPS results do not provide evidence for bulk RhO_x formation, partially oxidized Rh species may form to a small extent at the Rh-ceria interface. Obviously, this mechanism would still require relatively rapid migration of carbon from the interface to the rest of the Rh surface.

It should also be pointed out that Rh lies directly below Co and directly to the right of Ru in the periodic table and that both of these metals readily dissociate CO. This coupled with the fact that highly stepped surfaces of Rh exhibit some activity for CO dissociation (22,23) suggests that Rh is close to having the capability to dissociate CO. A reducible oxide support, such as ceria, may simply act to promote this tendency. It may well be that the degree of crystallinity of the ceria support influences the interaction with Rh due to differences in the extent of reduction of the support. For the highly crystalline ceria, the extent of ceria reduction in the immediate vicinity of the Rh may be greater, thus providing a larger promotional effect. There is at least some evidence to support this hypothesis. For example, it has previously been shown that polycrystalline ceria films release considerably more oxygen, and at lower temperatures, than do single crystals (16). This suggests that bulk reduction may be important for the polycrystalline materials, while only surface reduction plays a role for the more crystalline materials.

Whatever the correct explanation is for the high reactivity of Rh/ceria/YSZ, our results have several implications for the use of Rh/ceria catalysts. First, the dissociation of CO could provide an important deactivation mechanism for automotive emissions-control catalysts. While one would expect CO dissociation to be reversible, a catalyst which had the propensity to catalyze this reaction would likely have a higher light-off temperature and poorer performance as an oxidation catalyst. It should be noted that some catalyst formulations for automotive applications specify that ceria and Rh be separated from one another in the washcoat (26). Our results may provide a partial explanation for why this is desirable.

Although the interactions between Rh and ceria may be deleterious in automotive applications, the results of this study suggest that these interactions might be utilized to promote other reactions of interest. For example, dissociation of CO will be an important step in CO_2 reforming of methane and CO hydrogenation. Rh/ceria may also have interesting properties for other reactions.

SUMMARY

The results of this study demonstrate that adsorbed CO dissociates on YSZ-supported Rh/CeO_2 and that the fraction of CO which undergoes dissociation increases significantly as the CeO_2 surface is reduced. Isotopic labeling studies demonstrated that O atoms resulting from CO dissociation exchange rapidly with oxygen from ceria. CO dissociation was not observed on CeO_2-supported Pd or Pt, indicating that the metal–ceria interactions resulting in CO dissociation are Rh specific.

ACKNOWLEDGMENTS

This work was supported by the Department of Energy Office of Basic Energy Sciences Grant DE-FG03-85-13350 (RJG) and Grant DE-FG02-96ER14682 (JMV). Some facilities used in this work were also partially funded by the National Science Foundation through the MRSEC program (Grant DMR-963298).

REFERENCES

1. Otsuka, K., Hatano, M., and Morikawa, A., *J. Catal.* **79**, 493 (1983).
2. Fisher, G. B., Theis, J. R., Casarella, M. V., and Mahan, S. T., SAE Paper 931034 (1993).
3. Gandhi, H. S., and Shelef, M., *Stud. Surf. Sci. Catal.* **30**, 199 (1987).
4. Herz, R. K., and Sell, J. A., *J. Catal.* **94**, 199 (1985).
5. Bernal, S., Botana, F. J., Calvino, J. J., Cauqui, M. A., Cifredo, G. A., Jobacho, A., Pintado, J. M., and Rodriguez-Izquerido, J. M., *J. Phys. Chem.* **97**, 4118 (1993).
6. Cordatos, H., Bunluesin, T., Stubenrauch, J., Vohs, J. M., and Gorte, R. J., *J. Phys. Chem.* **100**, 785 (1996).
7. Stubenrauch, J., and Vohs, J. M., *J. Catal.* **159**, 50 (1996).
8. Stubenrauch, J., and Vohs, J. M., *Catal. Lett.* **47**, 21 (1997).
9. Dmowski, W., Egami, T., Gorte, R., and Vohs, J., *Physica B* **221**, 420 (1996).
10. Altman, E. I., and Gorte, R. J., *Surf. Sci.* **172**, 71 (1986).
11. Graham, G. W., *Surf. Sci.* **268**, 25 (1992).
12. Putna, E. S., Vohs, J. M., and Gorte, R. J., *Catal. Lett.* **45**, 143 (1997).
13. Roberts, S., and Gorte, R. J., *J. Chem. Phys.* **93**, 5337 (1990).
14. Zafiris, G. S., and Gorte, R. J., *J. Catal.* **132**, 275 (1991).
15. Zafiris, G. S., and Gorte, R. J., *J. Catal.* **139**, 561 (1993).
16. Putna, E. S., Vohs, J. M., and Gorte, R. J., *J. Phys. Chem.* **100**, 17862 (1996).
17. Creaser, D. A., Harrison, P. G., Morris, M. A., and Wolfindale, B. A., *Catal. Lett.* **23**, 13 (1994).
18. Stubenrauch, J., Ph.D. thesis, University of Pennsylvania, 1996.
19. Vannice, M. A., *J. Catal.* **40**, 129 (1975).
20. Doering, D. L., Poppa, H., and Dickinson, J. T., *J. Vac. Sci. Technol.* **17**, 198 (1980).
21. Ichikawa, S., Poppa, H., and Boudart, M., *J. Catal.* **91**, 1 (1985).
22. Castner, D. G., and Somorjai, G. A., *Surf. Sci.* **83**, 60 (1979).
23. Rebholz, M., Prins, R., and Kruse, N., *Surf. Sci.* **259**, L797 (1991).
24. Lavalley, J. C., Saussey, J., Lamotte, J., Breault, R., Hindermann, J. P., and Kiennemann, A., *J. Amer. Chem. Soc.* **94**, 5941 (1990).
25. Fierro, J. L. G., and Tejuca, L. G., *Appl. Surf. Sci.* **27**, 453 (1987).
26. Tomohisa, O., Tsuchitani, K., and Kitaguchi, S., Europ. Patent 89303729.1.